PREDICTION OF RESIDUAL STRESS FOR DISSIMILAR METALS WELDING AT NUCLEAR POWER PLANTS USING FUZZY NEURAL NETWORK MODELS

MAN GYUN NA*, JIN WEON KIM and DONG HYUK LIM
Department of Nuclear Engineering, Chosun University
375 Seosuk-dong, Dong-gu, Gwangju 501-759, Republic of Korea
*Corresponding author. E-mail : magyna@chosun.ac.kr

Received April 10, 2007
Accepted for Publication June 22, 2007

A fuzzy neural network model is presented to predict residual stress for dissimilar metal welding under various welding conditions. The fuzzy neural network model, which consists of a fuzzy inference system and a neuronal training system, is optimized by a hybrid learning method that combines a genetic algorithm to optimize the membership function parameters and a least squares method to solve the consequent parameters. The data of finite element analysis are divided into four data groups, which are split according to two end-section constraints and two prediction paths. Four fuzzy neural network models were therefore applied to the numerical data obtained from the finite element analysis for the two end-section constraints and the two prediction paths. The fuzzy neural network models were trained with the aid of a data set prepared for training (training data), optimized by means of an optimization data set and verified by means of a test data set that was different (independent) from the training data and the optimization data. The accuracy of fuzzy neural network models is known to be sufficiently accurate for use in an integrity evaluation by predicting the residual stress of dissimilar metal welding zones.

KEYWORDS : Dissimilar Metal Welding, Finite Element Analysis, Fuzzy Neural Network, Genetic Algorithm, Residual Stress, Subtractive Clustering.

1. INTRODUCTION

The factors that have an impact upon fatigue strength are residual stress, stress concentration, the mechanical properties of the material, and the macrostructure and microstructure. Residual stress is one of the most important factors but its effect on high-cycle fatigue is of more concern than the other factors. Residual stress is a tension or compression that exists in a material without any external load being applied, and the residual stresses in a component or structure are caused by incompatible internal permanent strains. Welding, which is one of the most significant causes of residual stress, typically produces large tensile stresses, the maximum value of which is approximately equal to the yield strength of materials that are joined by lower compressive residual stresses in a component. The residual stress of welding can significantly impair the performance and reliability of welded structures. The integrity of welded joints must be ensured against fatigue or corrosion during their long use in welded components or structures.

In particular, stress-corrosion cracking usually occurs when the following three factors exist at the same time: susceptible material, corrosive environment, and tensile stress (including residual stress). Thus, residual stress becomes very critical for stress-corrosion cracking when it is difficult to improve the material corrosivity of the components and their environment under operating conditions [1]. Since the welding residual stress is a major factor in the generation of primary water stress corrosion cracking (PWSCC), the prediction of the welding residual stress is important for preventing PWSCC.

Residual stresses may be measured by nondestructive techniques and locally destructive techniques. The nondestructive techniques include X-ray and neutron diffraction methods, magnetic methods, and ultrasonic techniques. The locally destructive techniques include hole drilling methods, ring core techniques, and sectioning methods. The selection of the optimum measurement technique should be based on consideration of the volumetric resolution, the material, the geometry, and the type of access.

In recent years, there has been a rapid increase in efforts to predict residual stresses by numerical modeling of welding processes. Modeling of welding is technically

and computationally demanding, and simplification and idealization of the material behavior, process parameters and geometry is inevitable. Numerical modeling is a powerful tool for predicting residual stress. Over the past fifteen years, the finite element method has been used to predict residual stress due to welding. Simulations of welding processes involve thermomechanical finite element analyses (FEAs) of the welding zone [2].

Artificial intelligence techniques, such as fuzzy inference systems and artificial neural networks, have recently been used as a powerful tool in a wide variety of nuclear engineering fields [3-9]. With training, fuzzy inference systems and neural networks can become adept at phenomenal nonlinear function approximation. We applied fuzzy neural networks (FNNs), which are characterized by the neuronal improvements of fuzzy systems and the fuzzification of neural network systems, to predict the residual stress due to welding. The aim of FNNs is to exploit the complementary nature of the two approaches: namely the fuzzy and neural network systems. By developing a finite element model for analyzing the residual stress and running the ABAQUS code [10], we acquired the training data, the optimization data, and the test data. Then, on the basis of the acquired data, we developed an FNN model to easily evaluate the residual stress in the welding of dissimilar metals for pipelines at nuclear power plants.

2. USE OF FINITE ELEMENT ANALYSES TO CALCULATE WELDING RESIDUAL STRESS

2.1 Analysis Condition

We conducted parametric FEAs to obtain the data on welding residual stress under various welding conditions. A dissimilar welding joint between a nozzle and a pipe is regarded in the analyses (see Fig. 1), because such joints are known to be highly susceptible to PWSCC in the primary systems of nuclear power plants. We assumed the base metals of the nozzle and the pipe to be SA508 ferritic steel and TP316 austenite stainless steel, respectively, and Alloy 82/182 was used as a filler metal. Next, a ferritic steel nozzle was buttered with Alloy 82 and treated with heat after the welding. We used a gas tungsten arc weld with the Alloy 82 filler metal in the first pass welding for the root gap, and then used a shielded metal arc weld with the Alloy 182 filler metal for the remaining passes.

The residual stress of a nozzle-pipe welding joint is usually influenced by pipe thickness, heat input, the strength of welding metals, and the constraints of welded pipes. We therefore used a combination of these parameters as input data in the parametric FEA. Table 1 summarizes the values of each parameter and the constraint conditions of the pipes.

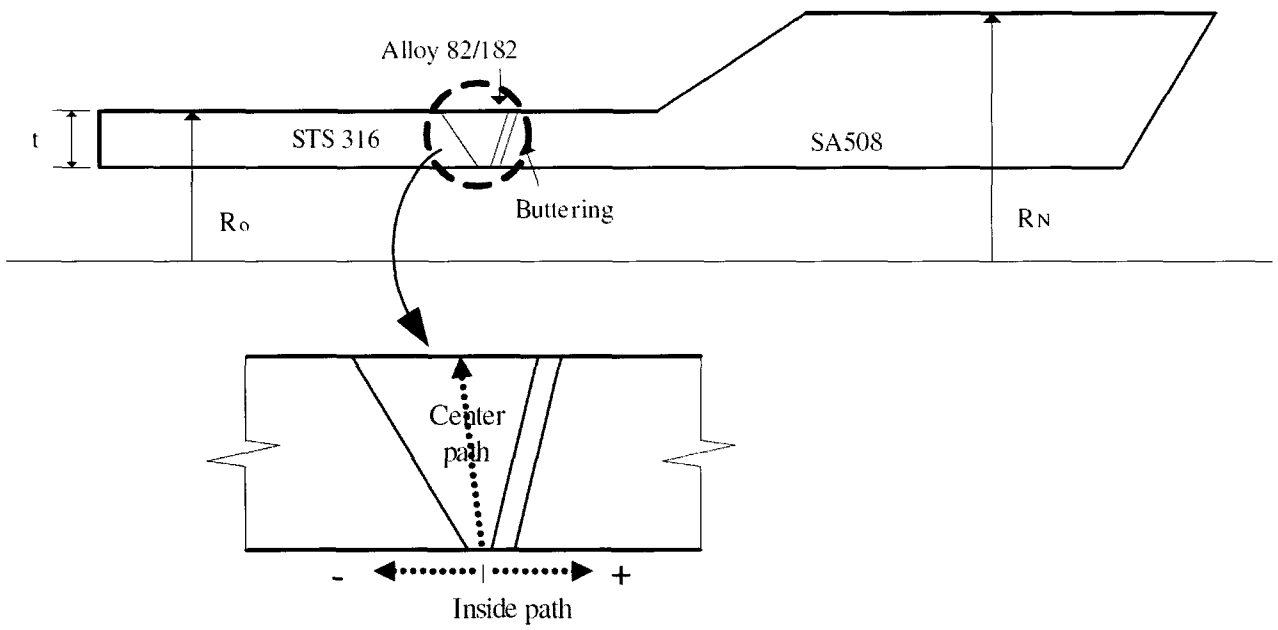

Fig. 1. A Welding Zone of Dissimilar Metals and Prediction Paths in the Welding Zone for Data Acquisition

2.2 Finite Element Models

In principle the simulation of finite element welding consists of a thermal analysis, which represents a thermal process during welding, followed by a structural analysis based on the results of the thermal analysis. We therefore used a sequentially coupled thermal-stress analysis to calculate the welding residual stress. For the structural analysis, we took the temperature contours, which were made available by the thermal analysis, and used them as input data to calculate a range of stress contours. For these analyses, we developed three types of axisymmetric two-dimensional finite element models, which, as shown in Fig. 2, vary in relation to the thickness of the pipes. Several studies have shown that an axisymmetric model is sufficient to simulate a pipe welding joint [11-13], even though real welding is a three-dimensional procedure. To calculate the welding residual stress, we used the ABAQUS program to perform the coupled FEAs [10]. We also used, as a finite element in the thermal analysis, an 8-node quadratic quadrilateral axisymmetric diffusive heat transfer (DCAX8 in ABAQUS); in addition, we used, as the element in the structural analysis, an 8-node biquadratic axisymmetric stress/displacement quadrilateral with reduced integration (CAX8R in ABAQUS).

The welding process was simulated by eight welding passes for $R_o/t = 8.8735$, nine welding passes for $R_o/t = 6.8763$, and 11 welding passes for $R_o/t = 4.8778$. Each bead in the model was considered to be a pass so that the number of passes in the finite element model was equal to the number of beads in the simulated welding. In the meshing, we identified each pass by grouping the corresponding elements and activating them incrementally to simulate the deposit of each bead. Given our assumption that post-welding heat treatment was conducted after the buttering, we ignored

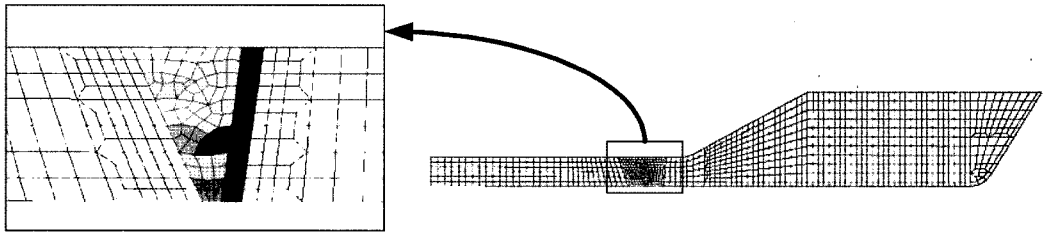

(a) $R_o/t = 4.8778$

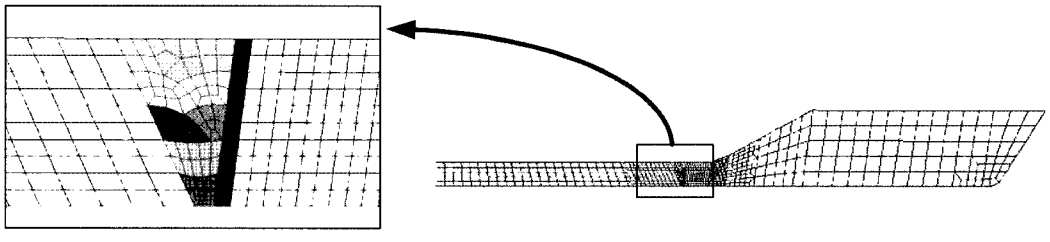

(b) $R_o/t = 6.8763$

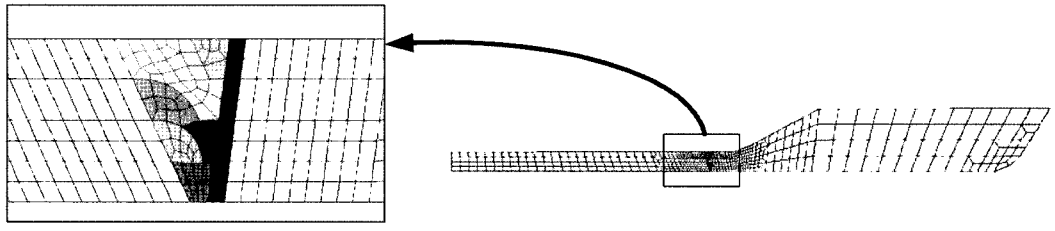

(c) $R_o/t = 8.8735$

Fig. 2. Axisymmetric Finite Element Models for a Nozzle-Pipe Dissimilar Metal Weld Joint

the buttering procedure in the models. We also ignored the metallurgical transformations in the ferritic steel; that is, in the heat-affected zone and with respect to the dilution between the base and welding metals. However, we did consider the annealing effect in the models, and the annealing temperature was 1400°C.

3. A FUZZY NEURAL NETWORK TO PREDICT WELDING RESIDUAL STRESS

In fuzzy inference modeling, it is relatively easy to set up rough fuzzy rules for a target system by intuition if we understand its dynamics well. However, the task of fine-tuning the fuzzy rules to improve modeling performance is difficult. We therefore propose an FNN that can embody fuzzy inference models. The proposed FNN provides functions for performing fuzzy inference. The functions can also be used to tune the parameters with respect to the shape of antecedent linguistic terms and the relative importance of rules.

3.1 A Fuzzy Inference Model

A fuzzy inference model consists of situation and action pairs where conditional rules described in *if-then* statements are generally used. The task of adapting fuzzy systems for on-line application involves neuronal improvements of fuzzy inference systems and the fuzzification of neural network systems. In this way we can exploit the complementary nature of fuzzy inference systems and neural network systems. The combination of the two systems is usually called an FNN system.

The fuzzy inference model can be accomplished through a clustering of numerical data. A cluster center is in essence a prototypical data point that exemplifies a characteristic behavior of a target system, and each cluster center can be used as the basis of a fuzzy rule that describes the system behavior. The development of a complete fuzzy system identification algorithm can therefore be based on the results of a subtractive clustering (SC) technique; this type of technique can be used as the basis of a fast and robust algorithm for identifying a fuzzy inference model [14]. We therefore present a fuzzy inference model based on an SC method, and the model can be used to predict the residual stress of dissimilar metal welding.

The data-based fuzzy inference model assumes the availability of N input/output training data pairs $(\mathbf{x}^T(k), y(k))$, where $\mathbf{x}^T(k) = (x_1(k), x_2(k), \cdots, x_m(k))$, $k = 1, 2, ..., N$. If we assume that the data points have been normalized in each dimension, the method can begin by generating a number of clusters in the $m \times N$ dimensional input space. To develop a systematic approach to the generation of fuzzy rules from a given input-output data set, we can use a Takagi-Sugeno-type fuzzy inference model [15], where the i-th fuzzy rule for the k-th time instant data is formulated as follows:

$$\begin{aligned} &\text{If } x_1(k) \text{ is } A_{i,1}(k) \ AND \ \cdots \ AND \ x_m(k) \text{ is } A_{i,m}(k), \\ &\text{then } \hat{y}_i(k) \text{ is } f_i\left(x_1(k), \cdots, x_m(k)\right), \end{aligned} \tag{1}$$

where $x_j(k)$ is the input linguistic variable to the fuzzy inference model ($j = 1, 2, ..., m$; m = the number of input variables), $A_{i,j}(k)$ is the membership function of the j-th input variable for the i-th fuzzy rule ($i = 1, 2, ..., n$; n = the number of rules), and $\hat{y}_i(k)$ is the output of the i-th fuzzy rule.

In the SC method, each data point is considered a potential cluster center and the SC method uses a measure of the potential of each data point, which is defined as a function of the Euclidean distances to all other input data points [14]:

$$P(k) = \sum_{j=1}^{N} e^{-4\|\mathbf{x}(k)-\mathbf{x}(j)\|^2/r_a^2}, \ k = 1, 2, ..., \mathrm{N}, \tag{2}$$

where r_a, which is the radius that defines the neighborhood, has considerable influence on the potential. The potential of a data point is high when it is surrounded by an abundance of neighboring data. After the potential of every data point has been computed, the data point with the highest potential is selected as the first cluster center, $\mathbf{x}_c(1)$. If $p_c(1)$ is the potential value of the first cluster center, the potential of each data point is revised by the following formula:

$$P(k) := P(k) - P_c(1)e^{-4\|\mathbf{x}(k)-\mathbf{x}_c(1)\|^2/r_b^2}, \ k = 1, 2, ..., \mathrm{N} \tag{3}$$

where r_b, another radius, is usually greater than r_a in order to limit the number of generated clusters. An amount of potential is subtracted from each data point as a function of its distance from the first cluster center. The data points near the first cluster center have greatly reduced potential and are therefore unlikely to be selected as the next cluster center. When the potentials of all data points have been revised according to Eq. (3), the data point with the highest remaining potential is selected as the second cluster center. In general, upon the determination of the i-th cluster center, $\mathbf{x}_c(i)$, the potential of each data point is revised in terms of the following equation:

$$P(k) := P(k) - P_c(i)e^{-4\|\mathbf{x}(k)-\mathbf{x}_c(i)\|^2/r_b^2}, \ k = 1, 2, ..., \mathrm{N}, \tag{4}$$

where $p_c(i)$ is the potential value of the i-th cluster center. If the inequality $P_c(i) < \varepsilon P_c(1)$ is true, these calculations stop; otherwise the calculations are repeated. The

parameter ϵ, which is a design parameter, controls the number of generated clusters, which corresponds to the number of fuzzy rules, n.

When the cluster estimation method is applied to a collection of input/output data, we can generate a number of n Takagi-Sugeno-type fuzzy rules, where the premise parts are fuzzy sets defined by the cluster centers that are obtained by the SC algorithm. The membership function value, $A_i(\mathbf{x}(k))$, of an input data vector, $\mathbf{x}(k)$, to the i-th cluster center, $\mathbf{x}_c(i)$, can be defined as follows:

$$A_i(\mathbf{x}(k)) = e^{-4\|\mathbf{x}(k)-\mathbf{x}_c(i)\|^2/r_a^2}. \tag{5}$$

The fuzzy inference model output, $\hat{y}(k)$, is calculated by the weighted average of the consequent parts of the fuzzy rules as follows:

$$\hat{y}(k) = \frac{\sum_{i=1}^{n} A_i(\mathbf{x}(k)) f_i(\mathbf{x}(k))}{\sum_{i=1}^{n} A_i(\mathbf{x}(k))}. \tag{6}$$

The function $f_i(\mathbf{x}(k))$ is a polynomial in the input variables, but it can be any function as long as it can appropriately describe the output of the fuzzy inference system within the fuzzy region specified by the antecedent of the rule. In the Takagi-Sugeno-type fuzzy inference model [15], the output of an arbitrary i-th fuzzy rule, f_i, is usually represented by the following first-order polynomial of inputs:

$$f_i(\mathbf{x}(k)) = \sum_{j=1}^{m} q_{i,j} x_j(k) + r_i, \tag{7}$$

where $q_{i,j}$ is a weighting value of the j-th input on the i-th fuzzy rule output and r_i is a bias of the i-th fuzzy rule output.

The output of the fuzzy inference model given by Eq. (6) can therefore be rewritten as

$$\hat{y}(k) = \sum_{i=1}^{n} \overline{w}_i(k) f_i(\mathbf{x}(k)) = \mathbf{w}^T(k)\mathbf{q}, \tag{8}$$

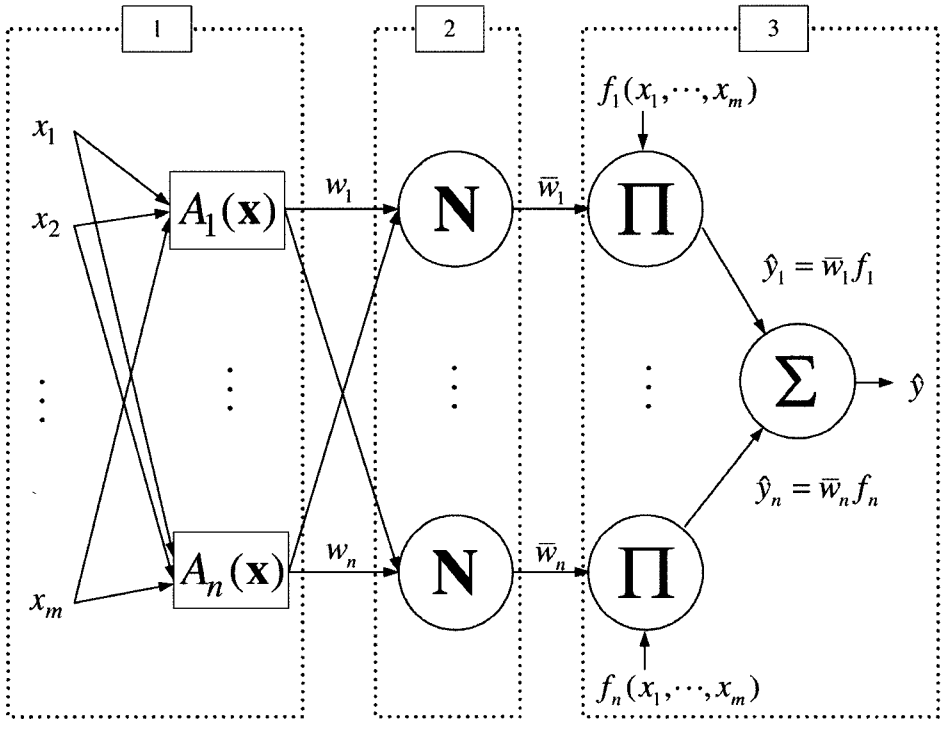

Fig. 3. A Fuzzy Neural Network Model

where

$$\bar{w}_i(k) = \frac{A_i(\mathbf{x}(k))}{\sum_{i=1}^{n} A_i(\mathbf{x}(k))},$$

$\mathbf{q} = [q_{1,1} \cdots q_{n,1} \cdots\cdots q_{1,m} \cdots q_{n,m}\, r_1 \cdots r_n]^T$, and

$$\mathbf{w}(k) = \left[\bar{w}_1(k)x_1(k)\cdots \bar{w}_n(k)x_1(k)\cdots\cdots \bar{w}_1(k)x_m(k)\cdots \bar{w}_n(k)x_m(k)\quad \bar{w}_1(k)\cdots \bar{w}_n(k)\right]^T,\ k = 1, 2, \cdots, N.$$

The value $\bar{w}_i(k)$ represents the normalized compatibility grade of the i-th fuzzy rule and consists of the input data and the normalized membership function values. The vector $\mathbf{q}$ is called the consequent parameter vector. Figure 3 describes the calculation procedure of the FNN model.

3.2 Training of the Fuzzy Inference Model

To attain the desired performance, we should optimize the fuzzy inference system by adapting the antecedent parameters (membership function parameters) and the consequent parameters (the polynomial coefficients of the consequent part). The adaptation methods of most fuzzy inference systems rely on the back-propagation algorithm [16]. The back-propagation algorithm is a general method for recursively solving parameter optimization but this conventional optimization algorithm is susceptible to getting stuck at local optima.

The genetic algorithm that has recently been widely used as an optimization method assumes the form of starting from many search points simultaneously climbing many peaks in parallel. A genetic algorithm is therefore less susceptible to being stuck at local minima than conventional search methods; conventional optimization methods, on the other hand, move from one point to another [17-18]. Moreover, the genetic algorithm is the most useful method of solving optimization problems with multiple objectives. However, because the genetic algorithm requires much computational time if there are many parameters involved, we can combine the genetic algorithm with a least squares algorithm to reduce the number of parameters that need to be optimized by the genetic algorithm. The genetic algorithm is used to optimize the cluster radii r_a and r_b as a means of generating the membership function through the SC of the numerical data; it also optimizes the other cluster radii of the SC (as explained in the next section) as a means of sampling the training data from all the acquired data. The least squares algorithm is used to calculate the consequent parameters $q_{i,j}$ and r_i.

In genetic algorithms, the term chromosome refers to a candidate solution that minimizes a cost function and the candidate solution is generally encoded as a bit string. The bit strings for each chromosome include the two cluster radii, r_a and r_b, for the membership function generation and other two cluster radii for sampling of the training data; note also that the bit strings are encoded with binary bits. As the generation proceeds, the chromosome populations are iteratively altered by biological mechanisms inspired by natural evolution, such as selection, crossover, and mutation.

The genetic algorithms require a fitness function that assigns a score to each chromosome (candidate solution) in the current population; they also maximize the fitness function value. The fitness function evaluates the extent to which each candidate solution is suitable for specified objectives. A root mean square (RMS) error and a maximum error can be a measure of the estimation performance of the FNN model. However, the minimization of the errors may only induce the overfitting in the FNN model, which means that the FNN model is a good fit for a specific data set (the training data) but not for another data set. We therefore divided the acquired data into three kinds of data sets: the training data, the optimization data, and the test data. The training data are used to solve the antecedent parameters and the consequent parameters of the FNN models. The optimization data are used to improve generalization capability of the FNN model by using another independent data set. We used the test data to verify the developed FNN models. Our specified multiple objectives were to minimize the RMS error along with the small maximum error as follows:

$$F = \exp(-\mu_1 E_1 - \mu_2 E_2 - \mu_3 E_3 - \mu_4 E_4), \tag{9}$$

where μ_1, μ_2, μ_3 and μ_4 are the weighting coefficients, and E_1, E_2, E_3 and E_4 have a concept of energy defined as

$$E_1 = \sqrt{\frac{1}{N_t}\sum_{k=1}^{N_t}\left(y_t(k) - \hat{y}_t(k)\right)^2}, \tag{10}$$

$$E_2 = \sqrt{\frac{1}{N_o}\sum_{k=1}^{N_o}\left(y_o(k) - \hat{y}_o(k)\right)^2}, \tag{11}$$

$$E_3 = \max_k \left\{ y_t(k) - \hat{y}_t(k) \right\}, \text{ and} \tag{12}$$

$$E_4 = \max_k \left\{ y_o(k) - \hat{y}_o(k) \right\}. \tag{13}$$

The variable $y(k)$ denotes the actual measured signal and the variable $\hat{y}(k)$ denotes the signal estimated by the FNN model. The subscripts t and o indicate the training data and the optimization data, respectively, and N_t and N_o represent the amount of training data and the optimization data.

If the antecedent parameters of the FNN model are fixed by the genetic algorithm, the output of the resulting FNN model can be described as a series of expansions of some basis functions. The basis function expansion is linear in its adjustable parameters, as shown in Eq. (8), because $\mathbf{w}^T(k)$ is known by the genetic algorithm. Thus, we can use the least squares method to determine the consequent parameters. The consequent parameter $\mathbf{q}$ was chosen to minimize the following cost function, including the squared error between the target output $\mathbf{y}$ and the estimated output $\hat{\mathbf{y}}$:

$$J = \sum_{k=1}^{N_t} \left(y(k) - \hat{y}(k) \right)^2 = \sum_{k=1}^{N_t} \left(y(k) - \mathbf{w}^T(k)\mathbf{q} \right)^2 = \frac{1}{2}(\mathbf{y} - \hat{\mathbf{y}})^2, \quad (14)$$

where

$\mathbf{y} = [y(1)\, y(2)\, \cdots\, y(N_t)]^T$ and

$\hat{\mathbf{y}} = \left[\hat{y}(1)\ \ \hat{y}(2)\ \cdots\ \hat{y}(N_t) \right]^T$.

The solution for minimizing the above cost function can be obtained by

$$\mathbf{y} = \hat{\mathbf{y}} = \mathbf{W}\mathbf{q}, \quad (15)$$

where

$$\mathbf{W} = \left[\mathbf{w}(1)\ \ \mathbf{w}(2)\ \cdots\ \mathbf{w}(N_t) \right]^T.$$

To solve the parameter vector $\mathbf{q}$ in Eq. (15), we should ensure that the matrix $\mathbf{W}$ is invertible but not usually a square matrix. We can easily solve the parameter vector $\mathbf{q}$ in Eq. (15) by using the pseudo-inverse of the $\mathbf{W}$ matrix as follows:

$$\mathbf{q} = \left(\mathbf{W}^T \mathbf{W} \right)^{-1} \mathbf{W}^T \mathbf{y}. \quad (16)$$

The parameter vector $\mathbf{q}$ can be calculated with a series of N_t input/output data pairs prepared for the training data.

4. APPLICATION

We initially developed a finite element model for analyzing welding residual stress. In the developmental process, we considered 150 analysis conditions, such as pipeline shapes, welding heat input, welding metal strength, and the constraints of the pipeline end parts, as a means of assessing the welding residual stress along two paths in the welding zone (as shown in Fig. 1). In addition, we used the ABAQUS code to calculate the welding residual stress at 21 locations along each path [10]. In total, as shown in Fig. 1, we acquired 6300 items of welding residual stress data from the two paths. Table 1 shows the conditions for analyzing the welding residual stress.

An FNN model can be well trained by using informative data. Input and output training data are excepted have many clusters, and the data at these cluster centers is more informative than neighboring data. Figure 4 shows data clusters and their centers (indicated with a plus sign) for simple two-dimensional data. We located the cluster centers with an SC scheme and used them as the training data set. The test data were selected every fifth data among the remaining data that the training data have been eliminated from all the acquired data. That is, the remaining data comprise 80 percent optimization data and 20 percent test data. The test data verifies the FNN model, independently of the training data and the optimization data. We used a genetic algorithm to optimize the FNN model as well as the SC selection algorithm for selecting the training data. The genetic algorithm parameters are the crossover probability, the mutation probability, and the population size. The values we used were 1 for the crossover probability, 0.05 for the mutation probability, and 20 for the population size.

We developed four FNN models for the two end-section constraints (restrained and free constraints) and two stress prediction paths (inside and center paths, as shown Fig. 1). The number of rules for the three fuzzy models was automatically determined by the SC method. To determine the antecedent parameters, such as the membership function parameters, we used the genetic algorithm to optimize the cluster radius and we used the least squares method to optimize the consequent parameters $q_{i,j}$ and r_i.

The FNN models were optimized with the training data and the optimization data and then tested with the test data. Tables 2 and 3 show the performance results of the FNN models. The relative RMS errors of the predicted residual stress are 4.0044% for the training data, 3.2745% for the optimization data, and 3.1011% for the test data. The FNN models have the best prediction performance for the restrained constraint and the inside path. Note also that the RMS errors of the FNN models for the test data are similar to the RMS errors for the training data and the optimization data, irrespective of

Table 1. Conditions for Analyzing Welding Residual Stress

Pipeline shape			Heat input, H [kJ/sec]	Yield stress of weld metal, σ_{ys} [MPa]	Constraint of end section
R_o [mm]	R_N [mm]	R_o/t	Pass 1; others		
			0.49764; 1.2690	192.33	
205.6	300.10	4.8778	0.55985; 1.4277	203.06	
205.6	271.75	6.8763	0.62205; 1.5863	213.70	Restrained
205.6	256.80	8.8735	0.68426; 1.7449	224.38	
			0.74646; 1.9036	235.07	
			0.49764; 1.2690	192.33	
205.6	300.10	4.8778	0.55985; 1.4277	203.06	
205.6	271.75	6.8763	0.62205; 1.5863	213.70	Free
205.6	256.80	8.8735	0.68426; 1.7449	224.38	
			0.74646; 1.9036	235.07	

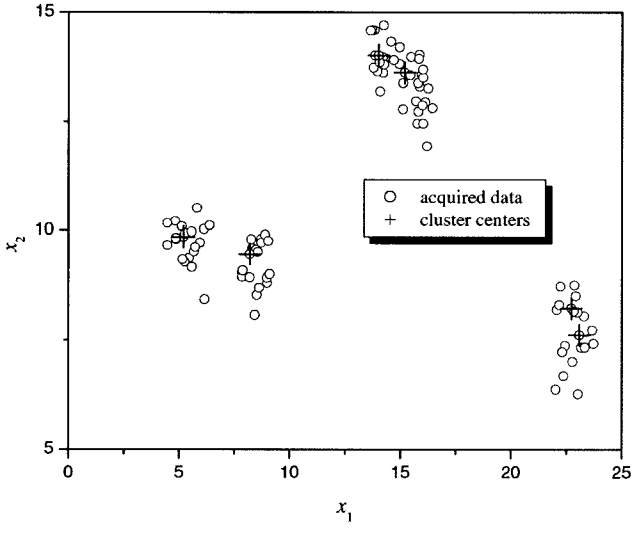

Fig. 4. Data Clusters and their Centers for Simple Two-Dimensional Data

the (restrained and free) constraints and the (inside and center) paths. Hence, if initially trained and optimized with the training data and the optimization data for a variety of welding conditions and pipeline shapes, the FNN models can accurately predict the welding residual stress for any other welding condition. The results confirm that the proposed FNN model favorably evaluates welding residual stress.

Figures 5 to 8 show the prediction performance of welding residual stress according to the prediction paths under two kinds of constraints at the end section, respectively. In these figures, the stress component is the Von Mises effective stress. The developed FNN model can predict welding residual stress with an RMS error level of less than 5% (as shown in Tables 2 and 3). Furthermore, the actual residual stress and the predicted residual stress are plotted for a specific welding condition of the end-section constraint, the heat input, and so forth. (Note also that the FEA data are assumed to be accurate.) In Figs. 5 to 8, the specific welding conditions are R_o/t = 4.8778, heat input = 0.62205 kJ/sec for the first welding pass and 1.5863 kJ/sec for other passes, and weld metal strength = 192.33 MPa (as shown in Table 1).

5. CONCLUSION

FNN models were developed for easy assessment of welding residual stress, which is important for maintaining the performance and reliability of welded structures, such as PWSCC. We applied the developed FNN models to numerical data obtained by means of FEAs. The acquired FEA data were divided into four data groups pertaining to the two end-section constraints and the two prediction paths. Thus, we used four fuzzy neural network models for two welding conditions and

Table 2. Performance of the Proposed FNN Model for the Welding Residual Stress Prediction (Inside Path)

Constraint of end section	Data type	RMS error (%)	Relative max error (%)	No. of data	Max. fitness
Restrained	Training data	2.0585	21.507	1261	0.9371
	Optimization data	3.2602	18.091	251	
	Test data	2.8432	13.706	63	-
Free	Training data	5.1301	35.567	1259	0.8504
	Optimization data	4.8382	25.899	252	
	Test data	4.1235	17.994	64	-

Table 3. Performance of the Proposed FNN Model for the Welding Residual Stress Prediction (Center Path)

Constraint of end section	Data type	RMS error (%)	Relative max error (%)	No. of data	Max. fitness
Restrained	Training data	4.5135	42.187	1261	0.9131
	Optimization data	2.9886	11.696	251	
	Test data	3.1258	16.949	63	-
Free	Training data	4.3153	38.571	1261	0.9384
	Optimization data	2.0108	7.212	251	
	Test data	2.3117	6.392	63	-

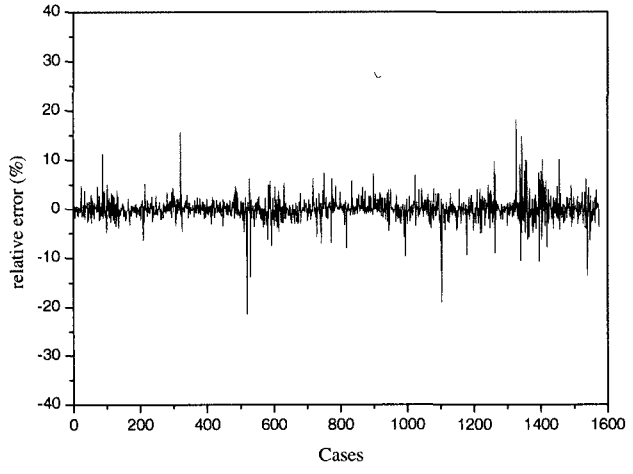

(a) Relative Error

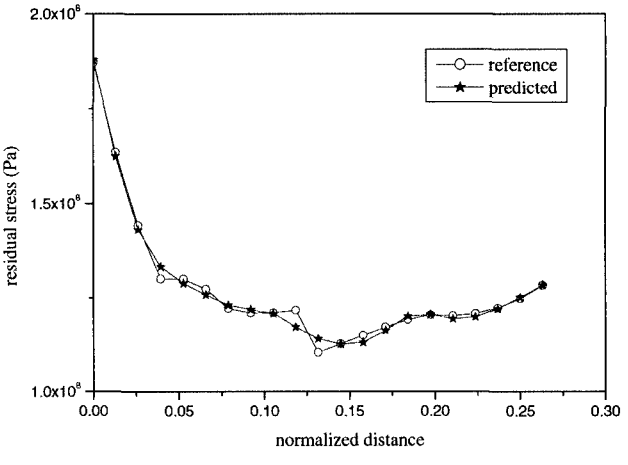

(b) Residual Stress Distribution for a Special Welding Condition

Fig. 5. Prediction Performance of Welding Residual Stress According to the Inside Path Under Restrained Constraint at the End Section

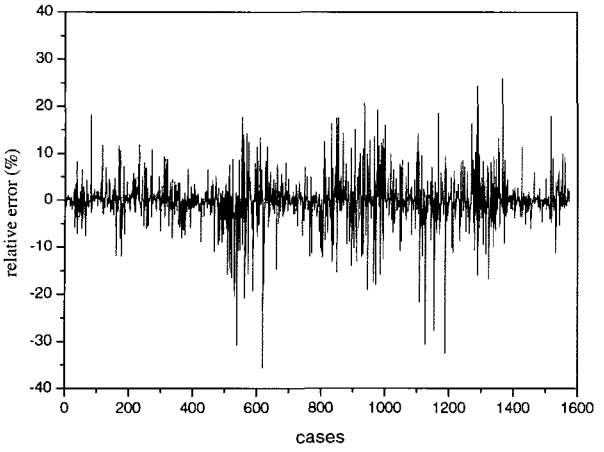

(a) Relative Error

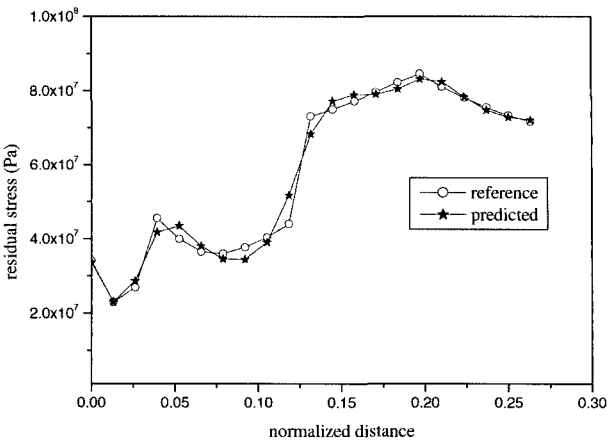

(b) Residual Stress Distribution for a Special Welding Condition

Fig. 6. Prediction Performance of Welding Residual Stress According to the Inside Path Under Free Constraint at the End Section

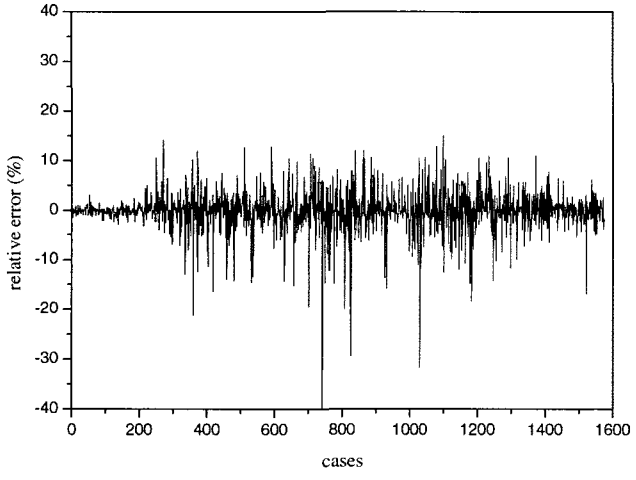

(a) Relative Error

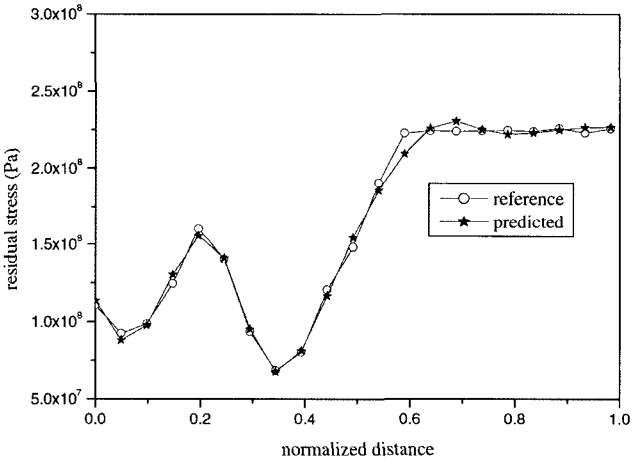

(b) Residual Stress Distribution for a Special Welding Condition

Fig. 7. Prediction Performance of Welding Residual Stress According to the Center Path Under Restrained Constraint at the End Section

two prediction paths. The FNN models were trained with the data set prepared for training (the training data), optimized with the optimization data set, and verified with the test data set, which differed from (or were independent of) the training data and the optimization data. The developed FNN model can predict welding residual stress with an RMS error level of less than 5%. The RMS errors of the FNN models for the test data are

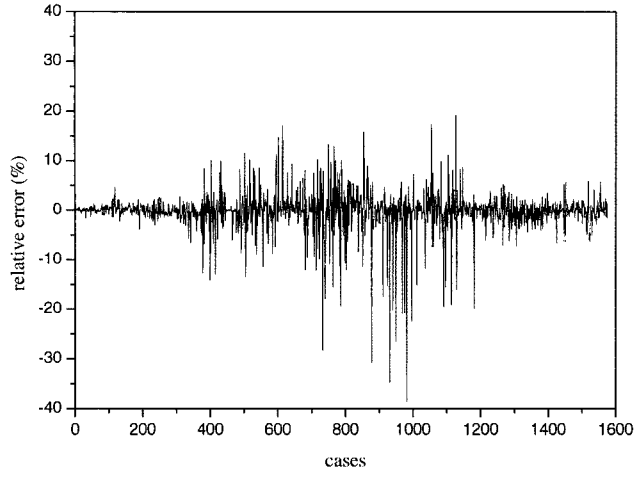

(a) Relative Error

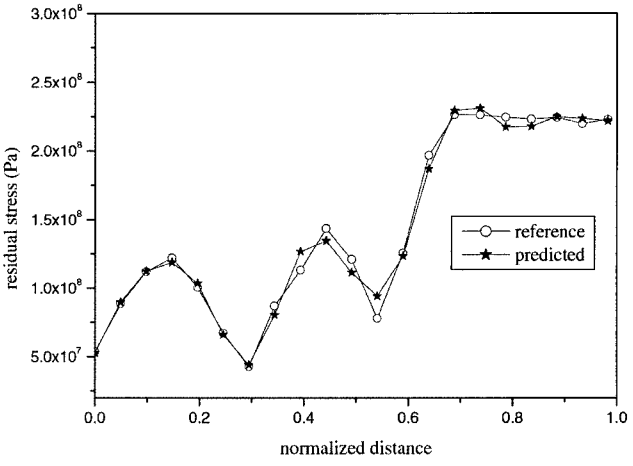

(b) Residual Stress Distribution for a Special Welding Condition

Fig. 8. Prediction Performance of Welding Residual Stress According to the Center Path Under Free Constraint at the End Section

less than the RMS error for the training data and the optimization data. Thus, if initially trained with a host of data, including a variety of welding conditions, the FNN models can accurately predict the welding residual stress for any other welding conditions. Our results confirm that the FNN models are sufficiently accurate to be used in the integrity evaluation of dissimilar metal welding zones.

REFERENCES

[1] M. Mochizuki, "Control of Welding Residual Stress for Ensuring Integrity Against Fatigue and Stress–Corrosion Cracking," *Nucl. Eng. Des.*, **237**, p. 107 (2007).

[2] P. Michaleris, J. Dantzig, and D. Tortorelli, "Minimization of Welding Residual Stress and Distortion in Large Structures," *Welding J.*, **78**, p. 361s (1999).

[3] E. B. Bartlett and R. E. Uhrig, "Nuclear Power Plant Diagnostics Using an Artificial Neural Network," *Nucl. Technol.*, **97**, p. 272 (1992).

[4] H. G. Kim, S. H. Chang, and B. H. Lee, "Optimal Fuel Loading Pattern Design Using an Artificial Neural Network and A Fuzzy Rule-Based System," *Nucl. Sci. Eng.*, **115**, p. 152 (1993).

[5] K. Kavaklioglu and B. R. Upadhyaya, "Monitoring Feedwater Flow Rate and Component Thermal Performance of Pressurized Water Reactors by Means of Artificial Neural Networks," *Nuclear Technology*, **107**, p. 112 (1994).

[6] J. W. Hines, D. J. Wrest, and R. E. Uhrig, "Signal Validation Using an Adaptive Neural Fuzzy Inference System," *Nucl. Technology*, **119**, p. 181 (1997).

[7] P. Fantoni, S. Figedy, and A. Racz, "A Neuro-Fuzzy Model Applied Full Range Signal Validation of PWR Nuclear Power Plant Data," *FLINS'98*, Antwerpen, Belgium, Sept. 14-16, 1998.

[8] M. G. Na and B. R. Upadhyaya, "A Neuro-fuzzy Controller for Axial Power Distribution in Nuclear Reactors," *IEEE Trans. Nucl. Sci.*, **45**, p. 59 (1998).

[9] M. G. Na, Dong Won Jung, Sun Ho Shin, Kibog Lee, and Yoon Joon Lee, "Estimation of the Nuclear Power Peaking Factor Using In-core Sensor Signals," *J. Korean Nucl. Soc.*, **36**, p. 420 (2004).

[10] Hibbitt, Karlson & Sorensen, Inc., *ABAQUS/Standard User's Manual*, 2001.

[11] V. Robin et al., "Modelling of Bimetallic Welds," *Proc. Mathematical Modeling of Weld Phenomena* 6, 2002.

[12] D. E. Katsareas and A. G. Youtsos, "Residual stress prediction in dissimilar metal weld pipe joints using finite element method," *Proc. ICRS-7*, 2004.

[13] B. Brickstad and B. L. Josefson, "A Parametric Study of Residual Stresses in Multi-Pass Butt-Welded Stainless Steel Pipes," *Int. J. of Press. Ves. & Piping*, **75**, p. 11 (1998).

[14] S. L. Chiu, "Fuzzy Model Identification Based on Cluster Estimation," *J. Intell. Fuzzy Systems*, **2**, p. 267 (1994).

[15] T. Takagi and M. Sugeno, "Fuzzy Identification of Systems and Its Applications to Modeling and Control," *IEEE Trans. Systems, Man, Cybern.*, **SMC-1**, p. 116 (1985).

[16] M. G. Na, Neuro-Fuzzy Control Applications in Pressurized Water Reactors: in Da Ruan (ed) *Fuzzy Systems and Soft Computing in Nuclear Engineering*, Springer-Verlag, Berlin Heidelberg New York, pp. 172-

207 (1999).
[17] D. E. Goldberg, *Genetic Algorithms in Search, Optimization, and Machine Learning*, Addison Wesley, Reading, MA (1989).
[18] M. Mitchell, *An Introduction to Genetic Algorithms*, MIT Press, Cambridge, MA (1996).